

Illuminating Metal-Ion Sensors: Benzimidazolesulfonamide Metal Complexes

David Martin, Matthieu Rouffet, and Seth M. Cohen*

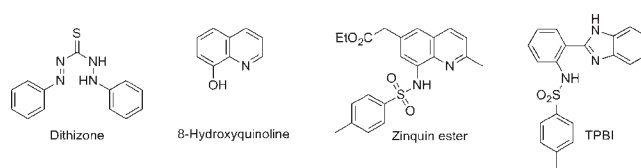
Department of Chemistry and Biochemistry, University of California, San Diego, La Jolla, California 92093, United States

Received August 20, 2010

The synthesis, structure, and solution spectroscopy of several (2-sulfonamidophenyl)benzimidazole metal complexes are reported. These ligands, which have been reported as selective molecular sensors for Zn^{2+} , readily form complexes with Co^{2+} , Ni^{2+} , Cu^{2+} , and Zn^{2+} . Surprisingly, the ligand adopts different binding modes depending on the metal ion. The work here provides insight into the coordination chemistry of these ligands, which may allow for the development of improved metal-ion sensors and metalloprotein inhibitors.

Despite much effort in trying to unravel the role of metal ions in biology, much remains to be learned about how metal cations are trafficked and stored prior to their incorporation into different metalloproteins.¹ Of particular interest is zinc, which is the second most abundant d-block metal ion in humans.² Historically, Zn^{2+} was detected using dithizone as a histochemical stain (Chart 1),¹ which revealed much about the spatial distribution of Zn^{2+} in various tissues. Today, fluorescent probes have attracted considerable attention for the direct visualization of biological Zn^{2+} at the molecular level. One of the first probes to be used was 8-hydroxyquinoline, which was further developed into Zinquin^{3,4} (Chart 1), a compound containing an 8-sulfonamidoquinoline core. The metal-binding properties and coordination chemistry of the 8-sulfonamidoquinoline motif have been well described in the literature. These compounds were found to show a strong increase in fluorescence upon binding Zn^{2+} . Later, Fahrni et al. developed Zn^{2+} -selective fluorescent sensors based on 2-(2'-tosylaminophenyl)benzimidazole (TPBI; Chart 1).⁵ These molecules absorb at ~300–340 nm and emit at ~400 nm (upon Zn^{2+} coordination), which may limit their use in vivo; however, they are attractive because they provide a

Chart 1. Compounds Used as Stains and Sensors for Zn^{2+}



ratiometric response, which allows for quantitative analysis of Zn^{2+} .⁵

In addition to Zn^{2+} -specific fluorescent probes, our laboratory has recently described the use of these zinc-binding motifs in the design of matrix metalloproteinase (MMP) inhibitors.⁶ It was found that several 8-sulfonamidoquinoline and (2-sulfonamidophenyl)benzimidazole fragments showed good activity and selectivity against several MMP isoforms. Despite the importance of metal binding in the activity of these compounds, there is essentially no information on the coordination chemistry of (2-sulfonamidophenyl)benzimidazole ligands to any metal ion. In this study, several benzimidazolesulfonamide metal complexes are reported, and their binding modes are directly compared to the well-documented 8-sulfonamidoquinoline analogues.

The TPBI ligand readily forms a variety of metal complexes under mild conditions. Co^{2+} , Ni^{2+} , and Zn^{2+} complexes were obtained by combining methanolic solutions of TPBI and a metal salt at room temperature. In the preparation of Ni^{2+} and Zn^{2+} complexes, the metal acetate salts were used and precipitation of the complexes was observed immediately. In the case of Co^{2+} , the nitrate salt was used, necessitating the addition of a base (Et_3N) for complex formation. To synthesize the Cu^{2+} complex, a methanolic TPBI solution was added to a yellow solution of $CuCl_2 \cdot 2H_2O$ in acetonitrile. Upon the addition of aqueous NaOH, the solution turned dark red, indicating formation of the complex. This Cu^{2+} complex did not precipitate out of the reaction mixture, so the solvents were removed under vacuum and the resulting residue was dissolved in acetone/ CH_2Cl_2 . The product was crystallized by vapor diffusion with diethyl ether as the precipitant.

UV–vis absorption spectra for the complexes are shown in Figure 1. In the UV region, $Zn(TPBI)_2$ has absorbance

(6) Rouffet, M.; de Oliveira, C. A. F.; Udi, Y.; Agrawal, A.; Sagi, I.; McCammon, J. A.; Cohen, S. M. *J. Am. Chem. Soc.* 2010, 132, 8232–8233.

*To whom correspondence should be addressed. E-mail: scohen@ucsd.edu.

(1) McRae, R.; Bagchi, P.; Sumalekshmy, S.; Fahrni, C. J. *Chem. Rev.* 2009, 109, 4780–4827.

(2) Nolan, E. M.; Lippard, S. J. *Acc. Chem. Res.* 2008, 42, 193–203.

(3) Nasir, M. S.; Fahrni, C. J.; Suhy, D. A.; Kolodsick, K. J.; Singer, C. P.; O'Halloran, T. V. *J. Biol. Inorg. Chem.* 1999, 4, 775–783.

(4) Fahrni, C. J.; O'Halloran, T. V. *J. Am. Chem. Soc.* 1999, 121, 11448–11458.

(5) Henary, M. M.; Wu, Y.; Fahrni, C. J. *Chem.—Eur. J.* 2004, 10, 3015–3025.

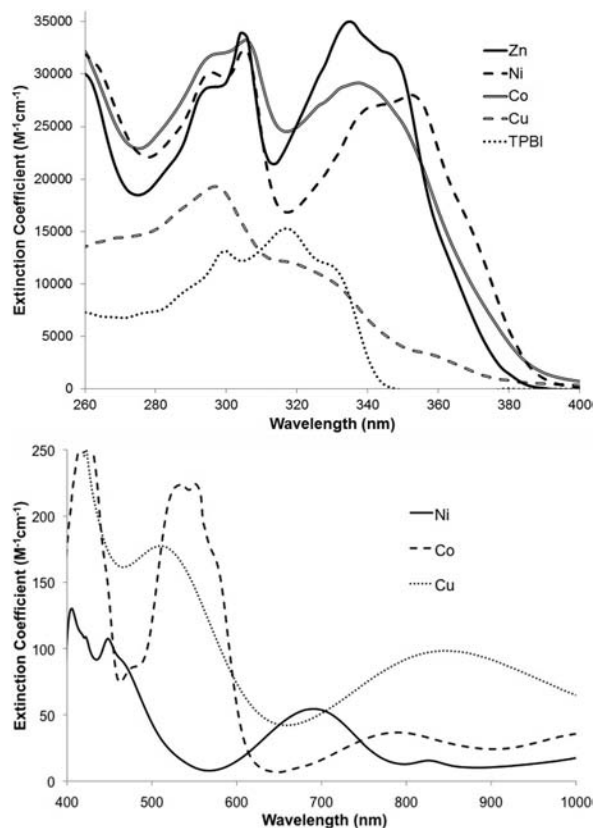


Figure 1. Top: Representative UV absorbance spectra of TPBI and its complexes. Bottom: Visible absorbance spectra of Ni(TPBI)₂, Co(TPBI)₂, and Cu(TPBI)Cl. All spectra were recorded in dimethyl sulfoxide.

maxima at 296 nm ($\epsilon = 29\,000\text{ M}^{-1}\text{ cm}^{-1}$), 304 nm ($\epsilon = 34\,000\text{ M}^{-1}\text{ cm}^{-1}$), and 334 nm ($\epsilon = 35\,000\text{ M}^{-1}\text{ cm}^{-1}$). The Co²⁺ and Ni²⁺ complexes also show maxima at 296 and 304 nm [Co(TPBI)₂, $\epsilon = 32\,000$ and $37\,000\text{ M}^{-1}\text{ cm}^{-1}$; Ni(TPBI)₂, $\epsilon = 30\,000$ and $32\,000\text{ M}^{-1}\text{ cm}^{-1}$]. In addition, Co(TPBI)₂ displays a transition at 338 nm and Ni(TPBI)₂ at 352 nm ($\epsilon \sim 29\,000\text{ M}^{-1}\text{ cm}^{-1}$ in both cases). Cu(TPBI)Cl shows only one transition at 296 nm ($\epsilon = 19\,000\text{ M}^{-1}\text{ cm}^{-1}$). The complexes are relatively weakly colored, as shown by their absorbance in the visible region of the spectrum. The red Co(TPBI)₂ complex is the most intensely colored, with maxima at 532 and 550 nm and extinction coefficients of 237 and $231\text{ M}^{-1}\text{ cm}^{-1}$, respectively. Co(TPBI)₂ also has a weak, broad absorbance centered at 790 nm ($\epsilon = 37\text{ M}^{-1}\text{ cm}^{-1}$). Cu(TPBI)Cl is also red, having an absorbance maximum at 510 nm ($\epsilon = 161\text{ M}^{-1}\text{ cm}^{-1}$) and a very broad absorbance centered at 840 nm ($\epsilon = 95\text{ M}^{-1}\text{ cm}^{-1}$) that trails into the visible region. The green Ni(TPBI)₂ complex has the faintest color, with absorbance maxima at 448 and 690 nm ($\epsilon = 109$ and $55\text{ M}^{-1}\text{ cm}^{-1}$, respectively). The fluorescence of the complexes was checked using a hand-held UV lamp (254 and 365 nm), and only Zn(TPBI)₂ emitted. Zn(TPBI)₂ was a strong emitter in aqueous solution at $\sim 415\text{ nm}$ when excited at 305 nm (data not shown).⁵

Single crystals of M(TPBI)₂ (M = Zn²⁺, Co²⁺, Ni²⁺) and Cu(TPBI)Cl were obtained, and their structures were determined by X-ray diffraction. Colorless blocks of Zn(TPBI)₂·2CHCl₃ crystallize in the monoclinic space group *C2/c*. The asymmetric unit consists of a deprotonated TPBI ligand bound by the imidazole and sulfonamide N atoms to a

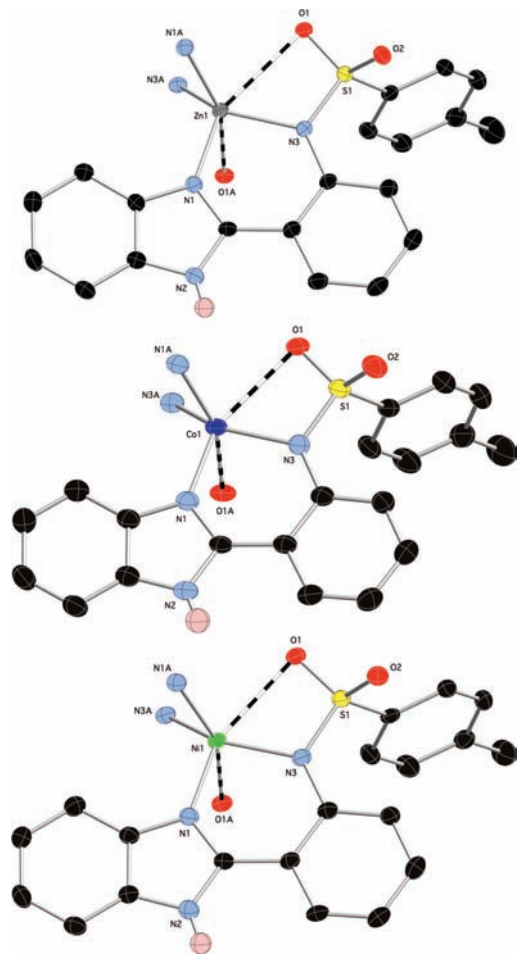


Figure 2. X-ray structural representations of Zn- (top), Co- (middle), and Ni(TPBI)₂ (bottom), with solvent molecules and H atoms (except for the imidazole N–H) removed for clarity. Only one complete TPBI ligand is shown for clarity. Thermal ellipsoids are shown at 50% probability.

Zn²⁺ ion with bond lengths of 2.005(2) and 1.978(2) Å, respectively (Figure 2). The complex cocrystallized with one CHCl₃ solvent molecule in the asymmetric unit. Extension of the inversion symmetry reveals a heavily distorted tetrahedral ZnN₄ coordination sphere, with N–Zn–N angles ranging from 92.05(7)° to 133.2(1)°. A long interaction between the Zn²⁺ ion and one of the sulfonamide O atoms may contribute to this distortion (Zn–O $\sim 2.70\text{ Å}$).

Red and green blocks of Co(TPBI)₂·2DMF and Ni(TPBI)₂·2DMF also crystallized in the space group *C2/c* with an asymmetric unit similar to that of Zn(TPBI)₂ but with the CHCl₃ solvent replaced by a *N,N*-dimethylformamide (DMF) molecule. The TPBI ligand adopts a binding mode similar to that in the Zn²⁺ complex (Figure 2). In Co(TPBI)₂, the Co–N distances are 1.981(3) and 1.992(3) Å for the sulfonamide and imidazole N atoms, respectively. The tetrahedral CoN₄ coordination is more distorted than that in the Zn²⁺ complex, with N–Co–N angles ranging from 91.5(1)° to 138.5(2)°. This increase in distortion is accompanied by a closer interaction between the Co atom and sulfonamide O atoms, with a Co–O bond length of 2.62 Å (Figure 2). The Ni–N bonds in Ni(TPBI)₂ are somewhat shorter at 1.962(2) and 1.981(2) Å for the sulfonamide and imidazole N atoms, respectively. The NiN₄ tetrahedron is even more distorted, having angles between 91.13(9)° and 143.68(14)° and a strong

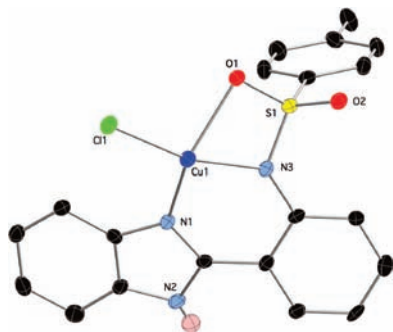


Figure 3. Asymmetric unit of Cu(TPBI)Cl, with H atoms (except for the imidazole N–H) removed for clarity. Thermal ellipsoids are shown at 50% probability.

interaction with the sulfonamide O atoms with a Ni–O distance of 2.57 Å.

Red blocks of Cu(TPBI)Cl crystallize in the triclinic space group $P\bar{1}$, with an asymmetric unit consisting of one Cu^{2+} ion bound by a single deprotonated TPBI ligand and a chloride ion (Figure 3). The Cu^{2+} ion adopts a distorted square-planar geometry consisting of the chloride ion, imidazole and sulfonamide N atoms, and, unlike the previous structures, a fully coordinated sulfonamide O atom. The Cu–N distances are much shorter than the M–N bonds in the other structures at 1.956(3) and 1.908(3) Å for the imidazole and sulfonamide N atoms, respectively. The Cu–O distance is 2.235(2) Å, and the Cu–Cl distance is 2.214(1) Å. The Cu^{2+} ion is coplanar with the Cl and N donors, with the O donor 17.6° out of the plane, as measured by the N–N–Cl–O torsion angle. Attempts to make a homoleptic Cu(TPBI)₂ complex with other metal sources such as nitrate, acetate, sulfate, and acetylacetonate were unsuccessful.

The primary structural difference between TPBI and the well-studied quinolinesulfonamide ligands (of the type used in Zinquin; Chart 1) is that, upon metal binding, TPBI forms a six-membered chelate, as opposed to a five-membered ring for the quinoline-based ligands. This causes the bite distance ($N_{\text{benz}}-N_{\text{amide}}$) to be ~0.2 Å larger, yielding $N_{\text{benz}}-M-N_{\text{amide}}$ bond angles that are roughly 10° wider than those in the 8-sulfonamidoquinoline complexes. The other consequence of the six-membered chelate is the closer positioning of the sulfonamide functionality to the metal, as observed by the $N_{\text{benz/quin}}-N_{\text{amide}}-S$ angle (~170° for quinoline-based

complexes compared to 150° for TPBI). Angling of the sulfonamide group toward the metal allows one of the O atoms to act as a weak donor, which is a feature not found in the structures of analogous quinoline-based complexes.^{3,7–23}

Many homoleptic complexes of quinolinesulfonamide ligands with Zn^{2+} and Cu^{2+} have been previously reported. The Zn^{2+} complexes do not differ significantly from the TPBI complex reported here, aside from those differences described above.^{3,8,11,12,14,15,23} In the case of Cu^{2+} , the ability of the TPBI ligand to supply a third donor deters the formation of a homoleptic complex, as found in previously reported structures with 8-sulfonamidoquinoline ligands.^{9,10,13,16–20} The metal adopts the favored square-planar geometry and avoids steric clashes between ligands by retaining a chloride ligand as its fourth donor. The more electron-deficient Co^{2+} and Ni^{2+} have complexes reported with two quinolinesulfonamide ligands, but the metals also ligate two solvent molecules (water or methanol) in order to adopt an octahedral geometry.^{7,21} Homoleptic complexes have only been reported by using bulkier 2,4-dimethylquinoline-²² and dimethylaminonaphthalenesulfonamide²⁴ ligands in order to deter the ligation of solvent molecules. In contrast, the TPBI ligand readily makes homoleptic complexes with these metals with donation from sulfonamide O atoms and the somewhat bulkier ligand framework. 2-(2,2-Sulfonamidophenyl)benzimidazole derivatives are promising fluorescence-based sensors for Zn^{2+} as well as potent leads for metalloproteinase inhibitors. The detailed coordination chemistry provided here will be essential to the development of the next generation of sensors and inhibitors based on these scaffolds.

Acknowledgment. We thank Dr. Y. Su for performing the mass spectrometry experiments. This work was supported by the NIH (Grant R21HL094571-01).

Supporting Information Available: X-ray crystallographic files in CIF format, synthetic and crystallographic details, and Table S1. This material is available free of charge via the Internet at <http://pubs.acs.org>. The atomic coordinates (CCDC reference numbers 789121–789124) for these structures have also been deposited with the Cambridge Crystallographic Data Centre. The coordinates can be obtained, upon request, from the Director, Cambridge Crystallographic Data Centre, 12 Union Road, Cambridge CB2 1EZ, U.K.

(7) Castresana, J. M.; Elizalde, M. P.; Arrieta, J. M.; Germain, G.; Declercq, J.-P. *Acta Crystallogr., Sect. C* **1984**, *40*, 763–765.

(8) da Silva, L. E.; Joussef, A. C.; Foro, S.; Schmidt, B. *Acta Crystallogr., Sect. E* **2006**, *62*, m1258–m1259.

(9) da Silva, L. E.; Joussef, A. C.; Foro, S.; Schmidt, B. *Acta Crystallogr., Sect. E* **2006**, *62*, m912–m913.

(10) da Silva, L. E.; Joussef, A. C.; Foro, S.; Schmidt, B. *Acta Crystallogr., Sect. E* **2006**, *62*, m518–m519.

(11) da Silva, L. E.; Joussef, A. C.; Foro, S.; Schmidt, B. *Acta Crystallogr., Sect. E* **2006**, *62*, m516–m517.

(12) da Silva, L. E.; Joussef, A. C.; Foro, S.; Schmidt, B. *Acta Crystallogr., Sect. E* **2006**, *62*, m1901–m1903.

(13) da Silva, L. E.; Joussef, A. C.; Foro, S.; Schmidt, B. *Acta Crystallogr., Sect. E* **2006**, *62*, m1606–m1608.

(14) da Silva, L. E.; Joussef, A. C.; Foro, S.; Schmidt, B. *Acta Crystallogr., Sect. E* **2006**, *62*, m1773–m1775.

(15) da Silva, L. E.; Joussef, A. C.; Foro, S.; Schmidt, B. *Acta Crystallogr., Sect. E* **2006**, *62*, m1719–m1721.

(16) Lim, M. H.; Lippard, S. J. *Inorg. Chem.* **2006**, *45*, 8980–8989.

(17) Macias, B.; Villa, M. V.; Garcia, I.; Castiñeiras, A.; Borrás, J.; Cejudo-Marin, R. *Inorg. Chim. Acta* **2003**, *342*, 241–246.

(18) Qiu, L.; Jiang, P.; He, W.; Tu, C.; Lin, J.; Li, Y.; Gao, X.; Guo, Z. *Inorg. Chim. Acta* **2007**, *360*, 431–438.

(19) Macias, B.; Villa, M. V.; Fiz, E.; Garcia, I.; Castiñeiras, A.; Gonzalez-Alvarez, M.; Borrás, J. *J. Inorg. Biochem.* **2002**, *88*, 101–107.

(20) Macias, B.; Villa, M. V.; Gómez, B.; Borrás, J.; Alzuet, G.; Gonzalez-Alvarez, M.; Castiñeiras, A. *J. Inorg. Biochem.* **2007**, *101*, 444–451.

(21) Macias, B.; Garcia, I.; Villa, M. V.; Borrás, J.; Castiñeiras, A.; Sanz, F. *Polyhedron* **2002**, *21*, 1229–1234.

(22) Fomina, I. G.; Sidorov, A. A.; Aleksandrov, G. G.; Mikhailova, T. B.; Pakhmotova, E. V.; Novotortsev, V. M.; Ikorskii, V. N.; Eremenko, I. L. *Russ. Chem. Bull.* **2004**, *53*, 1477–1487.

(23) Macias, B.; Garcia, I.; Villa, M. V.; Borrás, J.; Castiñeiras, A.; Sanz, F. *Z. Anorg. Allg. Chem.* **2003**, *629*, 255–260.

(24) Lim, M. H.; Kuang, C.; Lippard, S. J. *ChemBioChem* **2006**, *7*, 1571–1576.